ATMOSPHERIC CHEMISTRY

Black carbon lofts wildfire smoke high into the stratosphere to form a persistent plume

Pengfei Yu[1,2,3]*, Owen B. Toon[4,5], Charles G. Bardeen[6], Yunqian Zhu[5], Karen H. Rosenlof[2], Robert W. Portmann[2], Troy D. Thornberry[1,2], Ru-Shan Gao[2], Sean M. Davis[2], Eric T. Wolf[5,7], Joost de Gouw[1,8], David A. Peterson[9], Michael D. Fromm[10], Alan Robock[11]

In 2017, western Canadian wildfires injected smoke into the stratosphere that was detectable by satellites for more than 8 months. The smoke plume rose from 12 to 23 kilometers within 2 months owing to solar heating of black carbon, extending the lifetime and latitudinal spread. Comparisons of model simulations to the rate of observed lofting indicate that 2% of the smoke mass was black carbon. The observed smoke lifetime in the stratosphere was 40% shorter than calculated with a standard model that does not consider photochemical loss of organic carbon. Photochemistry is represented by using an empirical ozone-organics reaction probability that matches the observed smoke decay. The observed rapid plume rise, latitudinal spread, and photochemical reactions provide new insights into potential global climate impacts from nuclear war.

On 12 August 2017, wildfires in the Pacific Northwest produced a pyrocumulonimbus (pyroCb) event that injected smoke into the stratosphere (*1*, *2*). Although such injections have been observed previously (*3*), in this case the quantity of smoke injected was so large that it was observed in the stratosphere for more than 8 months, an unusually long time. Smoke particles from forest fires are largely composed of organic material (organic carbon, OC) and black carbon (BC). BC absorbs across the solar spectrum and heats the air. Part of OC, known as brown carbon, can absorb at blue and ultraviolet (UV) wavelengths but has a lifetime (e-folding time) as short as a few hours because it undergoes photochemical reactions (*4*). By contrast, BC is refractory and its light absorption is more persistent. Satellite observations show that the smoke ascended from its initial injection height near 12 to 23 km within 2 months. The ascent of smoke in the stratosphere by solar heating has been modeled previously (*5*–*7*), but in this case the distinctive plume rise was clearly observed by multiple observation platforms, allowing a rigorous test of model results.

[1]Cooperative Institute for Research in Environmental Sciences, University of Colorado, Boulder, CO, USA. [2]Earth System Research Laboratory, National Oceanic and Atmospheric Administration, Boulder, CO, USA. [3]Institute for Environment and Climate Research, Jinan University, Guangzhou, China. [4]Department of Atmospheric and Oceanic Sciences, University of Colorado, Boulder, CO, USA. [5]Laboratory for Atmospheric and Space Physics, University of Colorado, Boulder, CO, USA. [6]National Center for Atmospheric Research, Atmospheric Chemistry Division, Boulder, CO, USA. [7]Virtual Planetary Laboratory, Seattle, WA 98195, USA. [8]Department of Chemistry, University of Colorado, Boulder, CO, USA. [9]Naval Research Laboratory, Monterey, CA 93943, USA. [10]Naval Research Laboratory, Washington, DC 20375, USA. [11]Department of Environmental Sciences, Rutgers University, New Brunswick, NJ, USA.
***Corresponding author. Email: pengfei.yu@colorado.edu**

Climate model simulations of the smoke injection, coupled with satellite observations of the smoke plume's optical extinction, constrain the amount and characteristics of the injected smoke. We compare simulations of the smoke rise to observations to constrain the amount of BC in the smoke. The photochemistry of organic material in smoke in the stratosphere is uncertain (*8*, *9*). By comparing simulations of the longevity of the smoke in the stratosphere with observations, we can infer an effective reaction probability consistent with the observed decay of the 2017 pyroCb smoke. Once we establish that the model properly represents the quantity, rise rate, and destruction of the smoke, we use the model to demonstrate the impact on stratospheric temperature, ozone, and water vapor and infer how this relates to past studies on the impacts of large fires produced by nuclear weapons.

The smoke plume was observed by multiple remote-sampling instruments, including ground-based laser radars (lidars) (*1*) and operational and research satellites (*2*). Here, we compare numerical simulations with data from two highly sensitive satellite instruments: the Stratospheric Aerosol and Gas Experiment III on the International Space Station (SAGE III-ISS) (*10*) and the Cloud-Aerosol Lidar with Orthogonal Polarization (CALIOP) (*11*) on the Cloud-Aerosol Lidar and Infrared Pathfinder Satellite Observation (CALIPSO) satellite. SAGE III-ISS has made global stratospheric aerosol extinction measurements since June 2017, and CALIOP has provided high–spatial resolution backscatter profiles since 2006. In addition, we compare numerical simulations with data from the balloon-borne Printed Optical Particle Spectrometer (POPS) (*12*) that measured vertical profiles of the aerosol size distribution from Laramie, Wyoming (41.3°N, 105.6°W) on 9 November 2017 and 27 April 2018.

SAGE III-ISS aerosol extinction observations indicated that the smoke rose from 12 km on 12 August 2017 (the date of the pyroCb event) to 23 km within 2 months (Fig. 1 and fig. S1). A similar plume rise was shown by the aerosol backscatter measurements by CALIOP (fig. S2). After reaching its peak altitude, the smoke gradually descended with a subsidence rate of about 0.5 km per month (Fig. 1). During this period, the climatological large-scale motion is typically downward at mid- and high latitudes. One balloon-borne POPS (open triangle in Fig. 1) launched over Laramie, Wyoming, in November 2017 showed an enhanced aerosol layer in the 14- to 20-km range that is likely associated with the 12 August 2017 pyroCbs. Another POPS launched on 27 April 2018 found no discernible enhancement, suggesting that little or no residual smoke aerosol remained at that time. A more detailed comparison of those POPS launches is provided in fig. S3.

SAGE III-ISS aerosol extinction coefficients (km^{-1}) are shown by black boxes in Fig. 2A (all SAGE III-ISS data points are shown in fig. S4). In the first 2 months after the pyroCb injection, the observed extinction at 18 km spanned more than one order of magnitude, from background values of 0.9×10^{-4} to 1.4×10^{-4} km^{-1} (*13*) in regions devoid of smoke to values of 2×10^{-3} km^{-1} where smoke concentrations were at a maximum. In the following months, the smoke spread throughout the Northern Hemisphere (NH) stratosphere, and measured extinction coefficients became more spatially homogeneous. The aerosol extinction coefficient at 18 km slowly started to decrease in October 2017 but still remained elevated relative to background values even in April 2018 (Fig. 2A). Similar aerosol extinction coefficients at 18 km were found from the balloon-borne POPS measurements (Fig. 2A).

We used a sectional aerosol-climate model (14–16) (see supplementary materials) in association with multiple remote and in situ measurements to quantify the smoke mass distribution, the fraction of the smoke that is BC, and the effective heterogeneous reaction probability (γ) between smoke and ozone. From numerous simulations assuming different configurations of the OC/BC mixture, we found a "best estimate" for the initial particle mass injection from the pyroCb event of 0.3 Tg of carbonaceous aerosol mass with 2% BC and 98% organics emitted at 12- to 13-km altitude. The BC mass fraction is consistent with that measured in the smoke plume from the 2013 Rim Fire (*17*).

The rate of the smoke plume rise depends on the BC mass fraction within the smoke, because BC absorbs sunlight and heats the air parcel in which it resides. The absorption efficiency of BC is sensitive to the aerosol morphology, size, and mixing state. Given that the pyroCb smoke depolarized light by more than 20% (*18*, *19*), we hypothesize that the particles are solids composed of fractal aggregates of BC coated with organics (see details in the supplementary materials). The simulated plume rise rate from 12 to 23 km in our "best-estimate" case (2% BC in 0.3-Tg smoke)

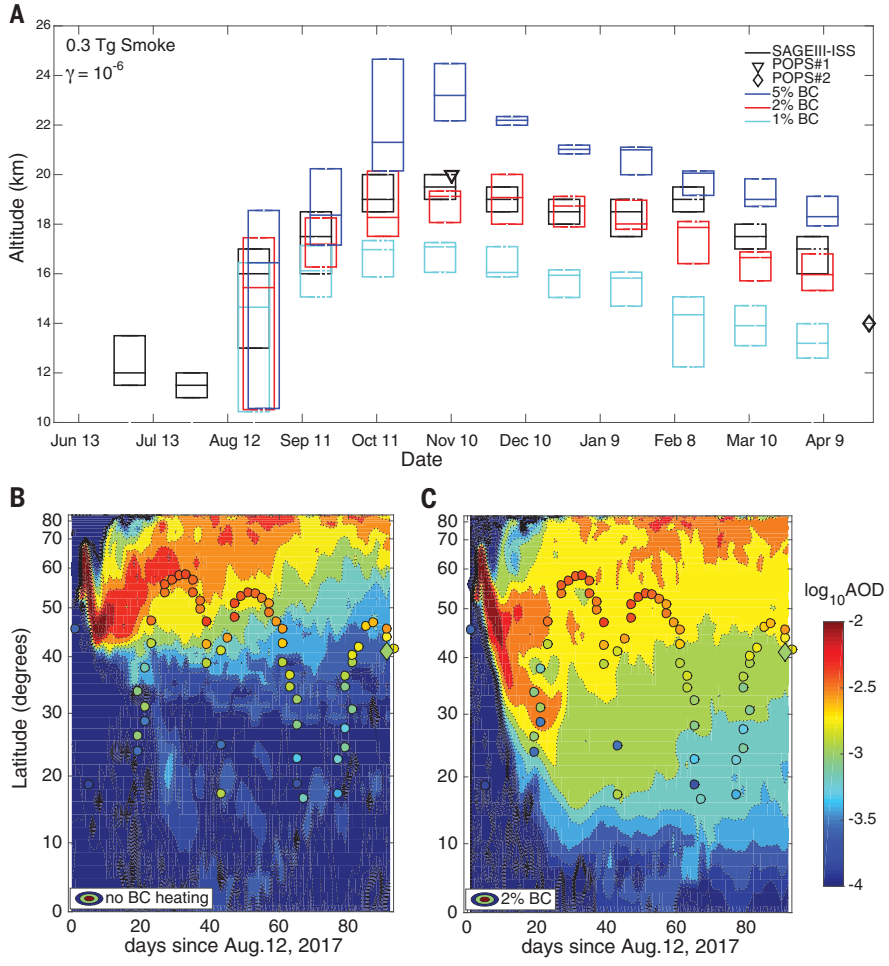

Fig. 1. Plume rise height changes with smoke composition. (**A**) Black boxes show SAGE III-ISS observations, and blue, red, and cyan boxes show climate model simulations with different fractions of black carbon (BC) in the smoke particles. Plume rise height observed by SAGE III-ISS and POPS (black open triangle and diamond) is defined as the maximum height where the aerosol extinction coefficient is greater than 1.5×10^{-4} km^{-1}, 50% higher than the background value in the lower stratosphere (*13*). SAGE III-ISS data are in the latitude range of 15° to 60°N, and simulations are plotted at the same locations as satellite observations. The upper, middle, and lower lines in each box denote the 25th, 50th, and 75th percentile of data, respectively. (**B**) Simulated latitudinal and temporal distribution of the stratospheric smoke AOD at 1020 nm without atmospheric heating from BC. Smoke AOD estimated from SAGE III-ISS (with background AOD before the fire starts subtracted) is denoted by colored circles. POPS measurement on 11 November 2017 is denoted by a diamond. (**C**) Same as (B) but with heating from BC. The smoke mass assumed in all simulations is 0.3 Tg with an effective ozone reaction probability of 10^{-6}. The best match between observations and calculations is with a BC fraction of 2%.

lies within the envelope of that estimated based on the SAGE III-ISS extinction (Fig. 1A) and CALIOP backscatter observations (fig. S2). The simulations plotted in Fig. 1A were sampled at the same times and locations as were the SAGE III-ISS observations. Additional simulations in Fig. 1A keeping the total smoke mass constant show that a plume with a BC mass fraction of 5% rises from 12 to 25 km in the first 2 months. By contrast, by using a lower BC mass fraction of 1%, the simulated smoke plume climbs to only 18 km.

The SAGE III-ISS aerosol optical depth (AOD) in the lower latitudes (15° to 30°N) was significantly higher than the background in the first month after the pyroCb event (Fig. 1, B and C). The simulation with the 2% BC generally reproduces the smoke AOD in the lower latitudes estimated by SAGE III-ISS and POPS measurements; however, the simulation without BC heating fails to transport enough smoke to the lower latitudes. Without BC (Fig. 1B), the smoke was quickly transported to polar regions where it was moved out of the stratosphere via the lower branch of the Brewer-Dobson circulation; however, the smoke with a small fraction of BC (e.g., 2%) can be lifted higher, extending its lifetime in the stratosphere.

The lifetime of the stratospheric smoke was observed to be ~150 days. The lifetime estimated from the standard model run without chemically active smoke is a dynamical lifetime. The dynamical lifetime only includes removal by transport and dilution by mixing, and is estimated to be ~ 250 days (Fig. 2B). Simulations show that the discrepancy between the observed and dynamical lifetime is likely due to the photochemical reactions that destroy organic particulate matter rather than the uncertainties from model-generated dynamics (fig. S5). Possible reactions include ultraviolet photolysis and heterogeneous reactions between organics and either ozone or the hydroxyl radical (OH). For simplicity, we use a one-step ozone-organic reaction in our model as a mathematical representation of all photochemical reactions. Figure 2A shows that calculated extinction in the "best-estimate" simulation with an effective reaction probability (γ) of 10^{-6} falls within the range of the extinction coefficients measured by SAGE III-ISS. Sensitivity simulations show that a higher γ value (10^{-5}) generates a smoke lifetime as short as 30 to 50 days (Fig. 2). The mass of organic material decays exponentially and the mass fraction of BC, which is not affected directly by the photochemical reaction, increases with time (fig. S6). OH has a limited impact on smoke lifetime in the lower stratosphere because the modeled OH reaction rate is a factor of 10 lower than that of ozone even with an effective γ of 1 (fig. S7). Photochemistry has a limited effect on smoke's latitudinal spread in the early stage (first month) as the chemical lifetime is about 6 to 8 months in the lower stratosphere.

Smoke warms the surrounding air and perturbs the spatial distributions of atmospheric trace species. One study simulating smoke plumes from fires triggered by detonation of nuclear weapons (*20*) found that BC produced in the fires contributes to stratospheric ozone destruction by heating the air and by transporting large amounts of water vapor into the upper stratosphere. We find that the August 2017 pyroCb smoke with only ~0.006 Tg of BC (2% of total injected mass) significantly perturbed the local vertical distribution of trace species. Figure 3 shows an ozone anomaly of <−0.3 parts per million by volume (ppmv) (about −50% at 100 mbar in the midlatitudes) observed by the Microwave Limb Sounder (MLS) (*21*) and Ozone Mapping Profiler Suite (OMPS) (*22*) corresponding with the plume location in August of 2017 as observed by CALIOP. In addition, a positive anomaly of H_2O (>5 ppmv) is observed by MLS. The simulation shows large ozone and water vapor anomalies consistent with observations (Fig. 3A). These anomalies in ozone and water vapor are a consequence of transport of tropospheric air into the stratosphere and are not due to in situ chemistry. The simulation predicts that the BC warms the local stratospheric air by up to 7 K in August 2017.

The 2017 pyroCb smoke plume remained detectable in the stratosphere for 8 months. Our simulations imply that the smoke had an initial

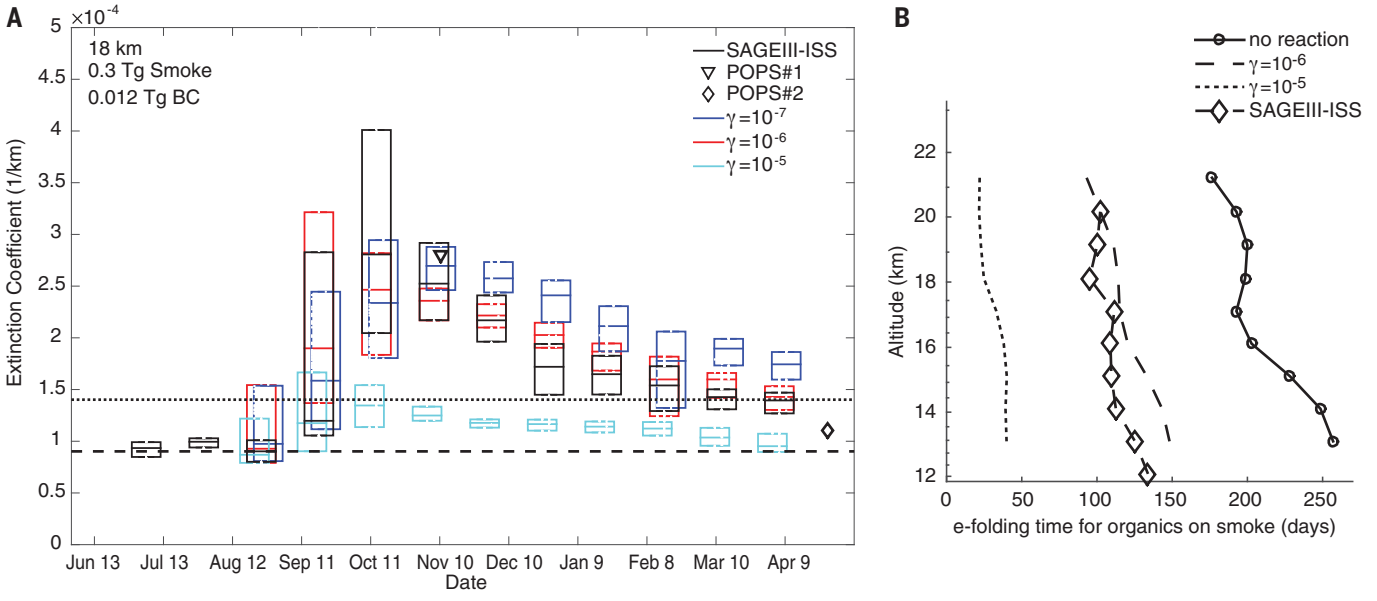

Fig. 2. Smoke extinction variation with effective ozone reaction probability (γ). (**A**) Aerosol extinction coefficient (km^{-1}) at 1020 nm with time at 15° to 60°N at 18 km observed by SAGE III-ISS (in black boxes) and modeled by CESM-CARMA (in colored boxes) with various γ of 10^{-5}, 10^{-6}, and 10^{-7}. Aerosol extinction coefficients at 1020 nm calculated from the size distributions measured by the two balloon-borne optical particle counters (POPS) launched over Laramie, Wyoming, are denoted by a black open triangle and diamond. Climatological mean aerosol extinction coefficient from satellites (*13*) during volcanic free period (2001 to 2005) and period with moderate stratospheric volcanic influence (2013 to 2016) are shown by black dashed and dotted lines, respectively. (**B**) Altitude-dependent lifetime with various values of γ (shown in solid, dashed, and dotted lines) for the smoke column optical depth above each altitude. Calculated smoke lifetime from SAGE III-ISS is shown by dashed line with diamond symbols.

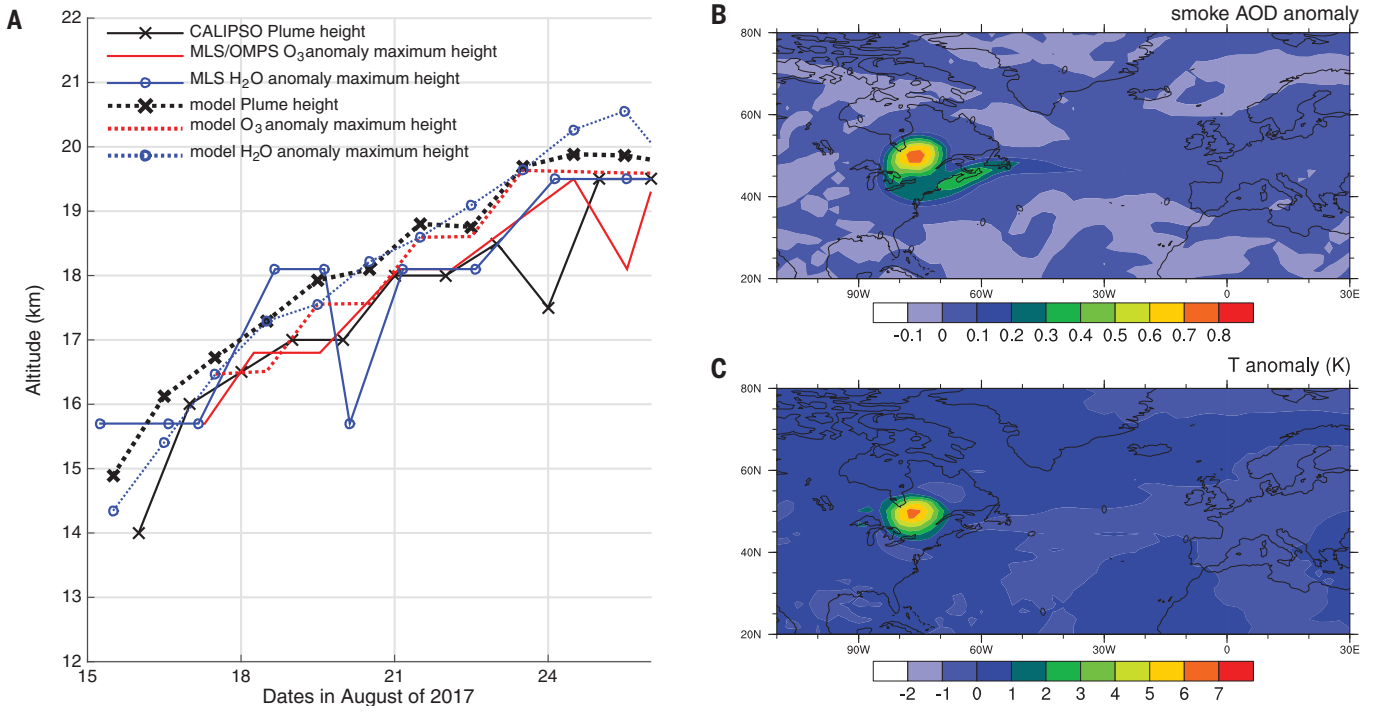

Fig. 3. Observed and modeled smoke transport in August 2017. (**A**) Maximum altitude of observed plume height by CALIOP in the region of interest in black lines with cross symbols; maximum altitude of observed significant O_3 negative anomaly (more negative than −0.3 ppmv) by MLS and OMPS in the region of interest (30° to 70°N, 80°W to 20°E) in red solid line; maximum altitude of observed water vapor positive anomaly (more than 5 ppmv) by MLS in the region of interest in blue lines with circle symbols; the same quantities simulated by CESM-CARMA are shown by colored dotted lines. (**B**) Modeled smoke AOD anomaly in mid-visible wavelengths on 21 August 2017. (**C**) Modeled temperature anomaly at 100 mbar between simulations with and without smoke on 21 August 2017.

organic mass fraction of 98%. Smoke lifetime is observed to be ~150 days in the stratosphere, which is 40% shorter than the modeled dynamical lifetime, suggesting that the photochemical lifetime of smoke particulate organic matter is fairly long. For a future large wildfire event, the chemical composition, size distribution, morphology, and photochemical reaction rates are important characteristics to measure to improve our predictability of the three-dimensional transport of the smoke both in the troposphere and stratosphere. One of the important predictions of numerous models of nuclear winter is that smoke injected into the upper troposphere from urban fires will self-loft high into the stratosphere (*5*–*7*, *23*, *24*). Estimates of BC injections from burning cities vary with the assumed fuel loads for each city but are typically about 0.05 Tg of BC per weapon for a wide range of scenarios (*25*, *26*). Our work shows that self-lofting will occur above a single set of fires and with an order-of-magnitude less BC than typical for urban fires. However, the observed rise from the 2017 fires to 23 km is much less than the rise predicted from the more BC-rich urban fires, whose smoke is predicted to rise to 50 km or more. Most nuclear winter studies have assumed that the organics in smoke can be ignored because of their rapid loss from photochemical reactions (*6*, *7*, *23*). This study calls that assumption into question given the observed persistence of the smoke in the 2017 fire plume.

REFERENCES AND NOTES

1. S. Khaykin *et al*., *Geophys. Res. Lett.* **45**, 1639–1646 (2018).
2. D. Peterson *et al*., *NPJ Clim. Atmos. Sci.* **1**, 30 (2018).
3. M. Fromm *et al*., *Bull. Am. Meteorol. Soc.* **91**, 1193–1210 (2010).
4. H. Forrister *et al*., *Geophys. Res. Lett.* **42**, 4623–4630 (2015).
5. R. C. Malone, L. H. Auer, G. A. Glatzmaier, M. C. Wood, O. B. Toon, *Science* **230**, 317–319 (1985).
6. A. Robock *et al*., *Atmos. Chem. Phys.* **7**, 2003–2012 (2007).
7. A. Robock, L. Oman, G. L. Stenchikov, *J. Geophys. Res.* **112**, D13107 (2007).
8. J. B. Burkholder *et al*., *JPL Publ.* 15–10 (2015).
9. J. A. de Gouw, E. R. Lovejoy, *Geophys. Res. Lett.* **25**, 931–934 (1998).
10. M. Cisewski *et al*., *Proc. SPIE* **9241**, 924107 (2014).
11. D. M. Winker *et al*., *J. Atmos. Ocean. Technol.* **26**, 2310–2323 (2009).
12. R. S. Gao *et al*., *Aerosol Sci. Technol.* **50**, 88–99 (2016).
13. L. Thomason *et al*., *Earth Syst. Sci. Data* **10**, 469–492 (2018).
14. P. Yu *et al*., *J. Adv. Model. Earth Syst.* **7**, 865–914 (2015).
15. C. G. Bardeen *et al*., *J. Geophys. Res. Atmos.* **118**, 11679–11697 (2013).
16. O. B. Toon, R. P. Turco, D. Westphal, R. Malone, M. S. Liu, *J. Atmos. Sci.* **45**, 2123–2144 (1988).
17. P. Yu *et al*., *J. Geophys. Res. Atmos.* **121**, 7079–7087 (2016).
18. Q. Hu *et al*., *Atmos. Chem. Phys.* **19**, 1173–1193 (2018).
19. M. Haarig *et al*., *Atmos. Chem. Phys.* **18**, 11847–11861 (2018).
20. M. J. Mills, O. B. Toon, R. P. Turco, D. E. Kinnison, R. R. Garcia, *Proc. Natl. Acad. Sci. U.S.A.* **105**, 5307–5312 (2008).
21. J. W. Waters *et al*., *J. Atmos. Sci.* **56**, 194–218 (1999).
22. N. A. Kramarova *et al*., *Atmos. Chem. Phys.* **14**, 2353–2361 (2014).
23. M. J. Mills, O. B. Toon, J. Lee-Taylor, A. Robock, *Earths Futur.* **2**, 161–176 (2014).
24. F. S. R. Pausata, J. Lindvall, A. M. L. Ekman, G. Svensson, *Earths Futur.* **4**, 498–511 (2016).
25. O. B. Toon *et al*., *Atmos. Chem. Phys.* **7**, 1973–2002 (2007).
26. O. B. Toon, A. Robock, R. P. Turco, *Phys. Today* **61**, 37–42 (2008).

ACKNOWLEDGMENTS

We thank J. Burkholder, D. W. Fahey, G. Mann, L. Liu, M. I. Mishchenko, G. Schill, J. Schwarz, and P. Campuzano-Jost for helpful discussions. The CESM project is supported by the National Science Foundation and the Office of Science (BER) of the U.S. Department of Energy. We acknowledge high-performance computing support from Cheyenne (doi:10.5065/D6RX99HX) provided by NCAR's Computational and Information Systems Laboratory, sponsored by the National Science Foundation. This work used the RMACC Summit supercomputer, which is supported by the National Science Foundation (awards ACI-1532235 and ACI-1532236), the University of Colorado Boulder, and Colorado State University. **Funding**: P.Y., R.W.P, K.H.R, S.M.D., and R.-S.G. are supported by NOAA ESRL CSD; O.B.T., A.R., C.G.B., and Y.Z. are supported by the Open Philanthropy Project; T.D.T. is supported by the NASA Upper Atmosphere Research Program, NOAA UAS Program and NOAA ESRL CSD; and D.A.P. is supported by the NASA New Investigator Program. **Author contributions:** P.Y., O.B.T., R.W.P., R.-S.G., and K.H.R. wrote the manuscript. P.Y., O.B.T., C.G.B., and A.R. designed the model experiments. P.Y. performed model simulations and analysis on SAGE III-ISS. P.Y. and Y.Z. analyzed the CALIOP data. C.G.B., O.B.T., P.Y, and E.T.W. performed the optical properties calculations. M.D.F. and D.A.P. provided meteorological details and initial analysis on the pyroCb smoke. T.D.T. and R.-S.G. provided the POPS measurements. P.Y. and S.M.D. performed analysis on MLS data. J.d.G. provided insights on ozone reaction and smoke morphology. All authors edited the manuscripts. **Competing interests:** The authors declare no competing interests. **Data and materials availability:** SAGE III-ISS data are available at https://eosweb.larc.nasa.gov/project/sageiii-iss/sageiii-iss_table; CALIOP data are available at https://eosweb.larc.nasa.gov/project/calipso/calipso_table; POPS data, model simulations and MSTM code are available at https://osf.io/efqd5/?view_only=09dca4c0903446fb831344bc4c87081a; MLS data are available at https://disc.gsfc.nasa.gov.

SUPPLEMENTARY MATERIALS

science.sciencemag.org/content/365/6453/587/suppl/DC1
Materials and Methods
Supplementary Text
Figs. S1 to S12
Table S1
References (*27*–*36*)

27 February 2019; accepted 12 July 2019
10.1126/science.aax1748